Histopathological findings and viral tropism in UK patients with severe fatal COVID-19: a post-mortem study

Brian Hanley, Kikkeri N Naresh, Candice Roufosse, Andrew G Nicholson, Justin Weir, Graham S Cooke, Mark Thursz, Pinelopi Manousou, Richard Corbett, Robert Goldin, Safa Al-Sarraj, Alireza Abdolrasouli, Olivia C Swann, Laury Baillon, Rebecca Penn, Wendy S Barclay, Patrizia Viola, Michael Osborn

Summary

Background Severe COVID-19 has a high mortality rate. Comprehensive pathological descriptions of COVID-19 are scarce and limited in scope. We aimed to describe the histopathological findings and viral tropism in patients who died of severe COVID-19.

Methods In this case series, patients were considered eligible if they were older than 18 years, with premortem diagnosis of severe acute respiratory syndrome coronavirus 2 infection and COVID-19 listed clinically as the direct cause of death. Between March 1 and April 30, 2020, full post-mortem examinations were done on nine patients with confirmed COVID-19, including sampling of all major organs. A limited autopsy was done on one additional patient. Histochemical and immunohistochemical analyses were done, and histopathological findings were reported by subspecialist pathologists. Viral quantitative RT-PCR analysis was done on tissue samples from a subset of patients.

Findings The median age at death of our cohort of ten patients was 73 years (IQR 52–79). Thrombotic features were observed in at least one major organ in all full autopsies, predominantly in the lung (eight [89%] of nine patients), heart (five [56%]), and kidney (four [44%]). Diffuse alveolar damage was the most consistent lung finding (all ten patients); however, organisation was noted in patients with a longer clinical course. We documented lymphocyte depletion (particularly CD8-positive T cells) in haematological organs and haemophagocytosis. Evidence of acute tubular injury was noted in all nine patients examined. Major unexpected findings were acute pancreatitis (two [22%] of nine patients), adrenal micro-infarction (three [33%]), pericarditis (two [22%]), disseminated mucormycosis (one [10%] of ten patients), aortic dissection (one [11%] of nine patients), and marantic endocarditis (one [11%]). Viral genomes were detected outside of the respiratory tract in four of five patients. The presence of subgenomic viral RNA transcripts provided evidence of active viral replication outside the respiratory tract in three of five patients.

Interpretation Our series supports clinical data showing that the four dominant interrelated pathological processes in severe COVID-19 are diffuse alveolar damage, thrombosis, haemophagocytosis, and immune cell depletion. Additionally, we report here several novel autopsy findings including pancreatitis, pericarditis, adrenal micro-infarction, secondary disseminated mucormycosis, and brain microglial activation, which require additional investigation to understand their role in COVID-19.

Funding Imperial Biomedical Research Centre, Wellcome Trust, Biotechnology and Biological Sciences Research Council.

Introduction

In the UK, the death toll from severe COVID-19 is among the highest worldwide.[1] Severe COVID-19 is characterised by respiratory failure, with so-called cytokine storm occurring in some patient subsets.[2] Pathological correlates are required to understand the pathophysiology of COVID-19. Autopsy-based histopathological analysis is crucial in this respect. In anticipation of the COVID-19 pandemic, our group produced national guidelines for autopsy performance in suspected COVID-19 cases.[3]

COVID-19 is caused by infection with severe acute respiratory syndrome coronavirus 2 (SARS-CoV-2).[4,5] Although SARS-CoV-2 and its predecessor SARS-CoV (causing severe acute respiratory syndrome [SARS]) are

similar on a molecular and clinical level, COVID-19 has a lower death rate (4% for COVID-19 vs 15% for SARS) and a substantially higher death toll (700 539 deaths worldwide from COVID-19 as of Aug 5, 2020 vs 774 from SARS) than SARS due to a higher basic reproduction number.[1] The post-mortem findings in patients with SARS-CoV infection included diffuse alveolar damage (DAD), splenic and nodal lymphocyte depletion, haemophagocytosis, renal acute tubular injury, cerebral oedema, micro-thrombosis, and adrenalitis with necrosis, with intracellular SARS-CoV detected in the lungs, kidney, brain, and haematological organs.[6] Various autopsy series on COVID-19 have begun to emerge in the literature.[7–15] Here, we document the major pathological

Department of Cellular Pathology, Northwest London Pathology (B Hanley MBBCh, Prof K N Naresh MD, C Roufosse PhD, J Weir FRCPath, Prof R Goldin MD, P Viola MD, M Osborn FRCPath) **and Department of Hepatology** (P Manousou PhD), **Imperial College London NHS Trust, London, UK; Centre for Haematology** (B Hanley, Prof K N Naresh) **and Centre for Inflammatory Diseases** (C Roufosse), **Department of Immunology and Inflammation, Department of Infectious Disease** (Prof G S Cooke FRCP, A Abdolrasouli PhD, O C Swann MRes, L Baillon BSc, R Penn MSc, Prof W S Barclay PhD), **and Department of Metabolism** (Prof M Thursz MD), **Faculty of Medicine, Imperial College London, London, UK; Department of Histopathology, Royal Brompton and Harefield NHS Foundation Trust and National Heart and Lung Institute, Imperial College London, London, UK** (Prof A G Nicholson DM); **Renal and Transplant Centre, Hammersmith Hospital, Imperial College Healthcare NHS, London, UK** (R Corbett PhD); **Department of Neuropathology, Kings College Hospital, London, UK** (Prof S Al-Sarraj FRCPath); **Death Investigation Committee, Royal College of Pathologists, London, UK** (M Osborn); **and Nightingale NHS Hospital, London, UK** (M Osborn)

Correspondence to:
Dr Brian Hanley, Department of Cellular Pathology, Northwest London Pathology, Charing Cross Hospital campus, London W6 8NA, UK
b.hanley@imperial.ac.uk

Research in context

Evidence before this study

COVID-19 is a new disease and comprehensive descriptions of the histopathological findings at autopsy are scarce. We reviewed the literature available on COVID-19 autopsy findings up to and including May 15, 2020. For this, we searched PubMed and Google Scholar databases with no language restrictions using the search terms "COVID-19", "SARS-CoV-2", "histology", "autopsy", and "post-mortem".

Added value of this study

Our series focused on providing a comprehensive description of the histopathological findings in patients with severe, fatal COVID-19 and correlating these findings with data on viral tropism. The most prominent findings included diffuse alveolar damage, thrombosis, haemophagocytosis, and immune cell depletion. Several novel autopsy findings in patients with COVID-19 were also described, including pancreatitis, pericarditis, adrenal micro-infarction, secondary disseminated mucormycosis, and brain microglial activation.

Implications of all the available evidence

Our study supports the existing clinical and autopsy literature that identified diffuse alveolar damage, thrombosis, immune cell depletion, and macrophage activation as the most prominent pathological features in COVID-19. Other factors, including acute kidney injury, pancreatitis, pericarditis, secondary fungal infections, and pre-existing liver disease, require further investigation. The presence of ongoing viral replication in late stage COVID-19 supports the continued use of antiviral therapy, even at a point in illness when immunopathology is dominant.

findings of ten post-mortem examinations done on patients with clinically confirmed COVID-19.

Methods

Patient selection

For this study, eligible patients were older than 18 years with premortem SARS-CoV-2 infection and COVID-19 listed clinically as the direct cause of death (under part 1 on the Medical Certificate of Cause of Death [MCCD]). Consent was obtained for all included patients according to the Human Tissue Authority 2009 codes of practice, by a member of the Trust Core Post-Mortem Consent Team. Consent rate was 52·6% (ten of 19 patients). Exclusion criteria included extended post-mortem interval before autopsy (>10 days) and patients with COVID-19 contributing, but not directly leading to death (under part 2 of the MCCD). Patients were from Imperial College National Health Service (NHS) Trust (nine patients; London, UK) and Royal Brompton & Harefield Foundation NHS Trust (one patient; London, UK). Premortem SARS-CoV-2 infection was identified using the Coronavirus Typing multiplex-tandem PCR High-Plex 24 System (Aus Diagnostics, Chesham, UK). Ethical approval for this project was provided by the Imperial College Healthcare Tissue Bank (R20012).

Autopsy procedures

Full autopsies were done on nine patients (PM1–9), and one patient underwent percutaneous biopsy sampling (heart, lungs, pancreas, kidneys, and liver) using percutaneous biopsy under ultrasound guidance (PM10). Full post-mortem examinations included standard sampling and were done according to Royal College of Pathologists guidelines.[3] Eight different regions of the brain were sampled for each full neuropathological examination. All tissue samples were fixed in formalin for a minimum of 72 h before embedding. Histochemical stains and immunohistochemistry were applied according to local protocols (appendix p 19). Organs were reviewed by subspecialist pathologists in lung (AGN and PV), haematopathology and immune pathology (KNN), liver (RG), gastrointestinal (MO), neuropathology (SA-S), and renal pathology (CR). Integrated interpretation was done by a subspecialty autopsy pathologist (BH and MO). All cases were reviewed independently by at least two pathologists.

PCR procedures

Fresh tissue for quantitative RT-PCR (qRT-PCR) analysis was processed within the biosafety level 3 facilities at St Mary's Hospital (London, UK), approved by the UK Health and Safety Executive and in accordance with local rules at Imperial College London. Total RNA was obtained from fresh tissue samples by use of TRIzol-chloroform extraction, followed by precipitation and purification using the RNeasy kit (Qiagen, Hilden, Germany). qRT-PCR against *E* gene, *RdRp*, and subgenomic RNA was done as described elsewhere.[16,17] In patient PM5, total fungal genomic DNA was extracted from four to five ribbon slices of a formalin-fixed, paraffin-embedded lung tissue block. Purified DNA was amplified with PCR for panfungal and Mucorales-specific targets.

Statistical analysis

All data was analysed using SPSS software, version 25, and expressed using median (IQR) and percentage.

Role of the funding source

The funder of the study had no role in study design, data collection, data analysis, data interpretation, or writing of the Article. The corresponding author had full access to all the data in the study and had final responsibility for the decision to submit for publication.

Results

Between March 1 and April 30, 2020, ten patients were included in the study. The median age at death was 73 years

(IQR 52–79). Seven (70%) of ten patients were men, three (30%) were women, and most patients were White or Asian (nine [90%]). Hypertension (four [40%] patients) and chronic obstructive pulmonary disease (three [30%]) were the most common contributing factors to death according to MCCD. All ten patients developed fever and had at least two respiratory symptoms or signs (cough, shortness of breath, reduced oxygen saturations, or pleuritic chest pain) during their early presentation. Of eight patients assessed for inflammatory markers, all (100%) had elevated inflammatory markers. These features were either apparent upon presentation to hospital (eight [80%] of ten patients) or developed in an inpatient (two [20%] patients, PM8 and PM9). Most patients died within 3 weeks of symptom onset (seven [70%] patients) and were not intubated or ventilated (six [60%] patients). Four patients were intubated during their presentation (PM2 for 7 days, PM5 for 22 days, PM6 for less than 1 day, and PM7 for 13 days). The median body-mass index (BMI) was in the obese range (31·2, IQR 22·3–40·0) and more patients were obese according to BMI at post mortem (five [56%] of nine) than indicated on the MCCD (one [10%] of ten). The median interval between death and post-mortem examination was 6 days (IQR 4·8–7·0), although the limited post mortem had a shorter interval (less than 20 h after death). Detailed clinical case vignettes are available in the appendix (p 3), and clinical data are summarised also in the appendix (p 20).

All patients had DAD: six showed purely exudative phase DAD and four showed a mixture of exudative and organising DAD (appendix p 22, figure 1). Three of four patients with organising-phase DAD had spent a substantial period on a ventilator (6 days, 12 days, and >20 days). Florid acute bronchopneumonia and ventilator-associated pneumonia were not noted in this series, although mild interstitial neutrophilic inflammation (three [30%] of ten patients) and patchy acute bronchopneumonia (three [30%] patients) were observed. Interstitial macrophages were prominent.

Macrophages were accompanied by scattered plasma cells. Mild or moderate lymphocyte inflammation was present in all ten patients, although focal lymphocyte cuffing of small vessels was noted in six patients (60%). We noted that lymphocytes in the lung were predominantly CD4-positive T cells. CD56-positive natural killer cells were rarely found. Occasionally, a patient had small aggregates of small B cells. Chronic bronchiolitis was seen in most patients (nine [90%] of ten). No granulomas or viral inclusion were seen. Invasive mucormycosis was noted in one patient (PM5, figure 1) and confirmed with Mucorales-specific PCR. The mucormycosis was vasculocentric and disseminated, involving the hilar lymph nodes, heart, brain, and kidney in the same patient.

Macroscopic (two [23%] of nine patients) and microscopic (eight [89%] of nine) pulmonary thromboemboli were frequent observations (appendix p 22, figure 2). Both fibrin-rich and platelet-rich thrombi were identified in small-sized and medium-sized vessels and within the

capillaries in alveolar septa (figure 2). External examination findings of deep venous thrombosis were not noted. Very focal lymphocytic vasculitis was identified in one patient.

Thrombotic features were universal in this cohort and all nine patients who underwent a full autopsy had at least one micro-thrombosis or macro-thrombosis in a major organ. One (11%) of nine patients had a macroscopic acute coronary thrombosis in the right coronary artery, whereas five patients (56%) had thrombi in the microcirculation of the heart on histological analysis. Coronary artery disease was negligible or mild in most patients (seven [78%] of nine). Acute myocardial ischaemic damage (<24 h old) was noted in the patient with an acute coronary artery thrombus (figure 2A, PM1). A mottled myocardium and subendocardial contraction band necrosis was noted in a
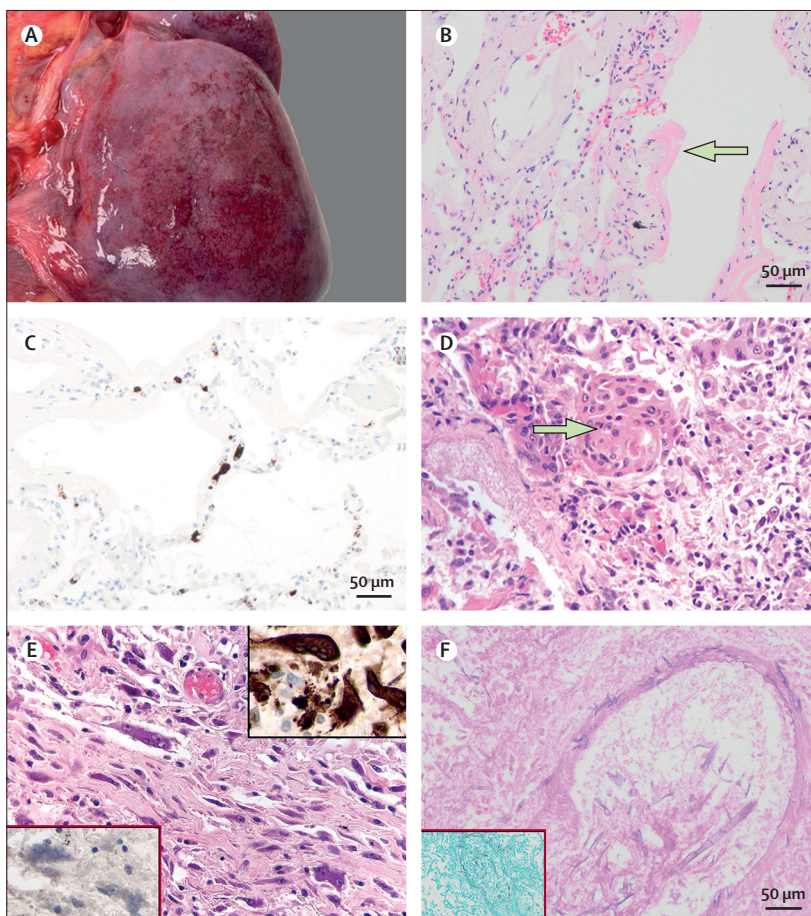

Figure 1: **Pulmonary pathological findings in patients with COVID-19**
(A) Macroscopic subpleural petechial haemorrhage in a 24-year-old man (PM6). (B) Hyaline membranes indicative of exudative phase diffuse alveolar damage in a 79-year-old woman (PM9) at 20x magnification.
(C) CD61 immunohistochemical staining indicating platelet-rich microthrombosis in alveolar capillaries (PM6).
(D) Squamous metaplasia in a 61-year-old man (PM1) with exudative phase diffuse alveolar damage at 40x magnification. (E) Interstitial multinucleated giant cells in a 79-year-old man (PM7) with organising phase diffuse alveolar damage at 40x magnification; the top right insert is of multinucleated giant cells showing positive CD68 staining, indicative of macrophage lineage; the bottom left insert shows absence of staining for cytokeratins.
(F) Periodic acid Schiff staining indicating wide, irregular, aseptate, and ribbon-like hyphae with open-angle branching and a vasculocentric pattern indicative of mucormycosis in a 22-year-old man (PM5); the insert is a Grocott silver stain highlighting mucormycosis at 20x magnification.

second patient (PM2); whether the contraction band necrosis was related to ischaemia or inotropic medication received in the intensive care unit is uncertain (appendix p 28). PM1 and PM2 were the two patients with the highest active viral load detected in the heart. A single pat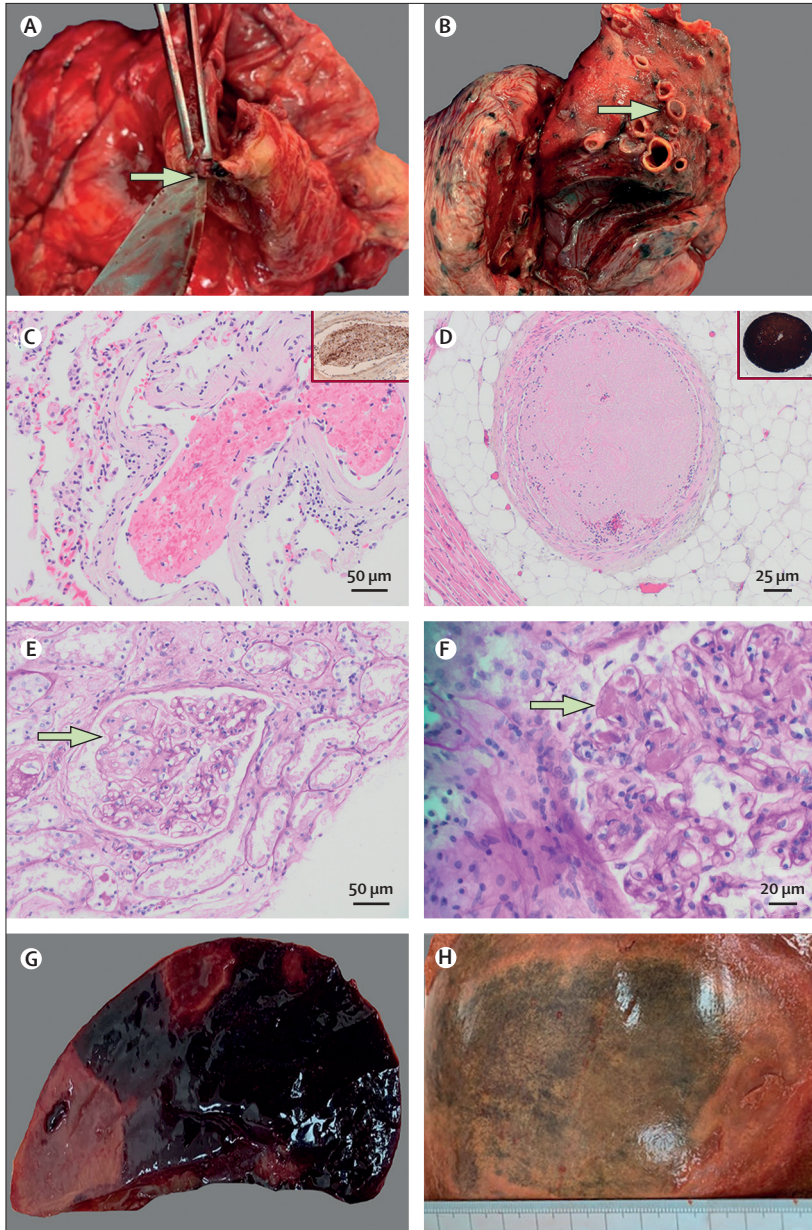ient (11%) had a right atrial thrombus. Pericarditis was identified in two patients (22%); one patient showed florid fibrinous pericarditis containing fungal hyphae (PM5), while the other showed only microscopic acute pericarditis (appendix p 22, figure 3). The median heart weight was high (450 g) and four (44%) of nine patients had left ventricular hypertrophy. Non-bacterial thrombotic (marantic) endocarditis was noted in one patient (PM5) with no known history or autopsy findings consistent with malignancy or chronic disorder associated with non-bacterial thrombotic (marantic) endocarditis (appendix p 22, figure 2). PM5 had disseminated mucormycosis and numerous other thrombotic features (appendix p 3). Cardiac amyloidosis and right atrial thrombosis were identified in one (10%) of ten patients (PM8; appendix p 28).

Lymphocyte depletion involving specific compartments and increased phagocytosis were prominent findings (appendix p 24, figure 4). Increased phagocytosis of other cells was identified in the sinusoidal macrophages of the red pulp of the spleen (in four [57%] of seven patients), sinus histiocytes of hilar lymph nodes (in three [50%] of six), and bone marrow (four [50%] of eight). Phagocytosis was identified in at least one of these organs in six (67%) of nine patients. Bone marrow haemophagocytosis was prominent in two patients (PM4 and PM8) and focal in two patients (PM7 and PM9). Depletion of periarteriolar T-cell sheaths within the white pulp was observed (figure 4). Red pulp was generally congested, showing reduced numbers of CD8-positive T cells. Plasma cells were variably prominent, and sinusoidal histiocytes showed phagocytosis of red blood cells and other cells to varying extents. Both IgM-positive and IgG-positive plasma cells were identified, and they were polytypic for light-chain expression (figure 4). Lymph nodes showed preservation of follicles and relative depletion of paracortical areas. Medullary areas showed prominence of plasma cells, and histiocytes were prominent in the sinuses. Bone marrow samples showed reactive changes with trilineage hyperplasia, and prominence of plasma cells and histiocytes were a common finding. A necrotising granuloma was noted in a single hilar lymph node in one patient, and acid-fast bacilli were noted on Ziehl Neelson staining (appendix p 28). All spleen and lymphoid material examined with immunohisto-chemistry were negative for Epstein-Barr virus and cytomegalovirus.

Pancreatitis was noted in two (25%) of eight patients. PM5 was a 22-year-old man with frank necrotic-haemorrhagic pancreatitis and secondary mucormycosis (figure 3). No fungal hyphae were noted in the pancreas. PM8 was a 97-year-old man who showed no substantial macroscopic pancreatitis, although microscopic acute inflammation within the pancreas and periadrenal fat necrosis was noted (figure 3). A third of patients (three [33%] of nine) showed patchy areas of infarct-type adrenocortical necrosis, with one patient showing organising microthrombi in adrenal vessels (figure 3). No

Figure 2: Thrombotic features identified at autopsy in patients with COVID-19
(A) Macroscopic right coronary artery thrombosis (arrow) in a 61-year-old man (PM1) with exudative phase diffuse alveolar damage. (B) Macroscopic pulmonary thromboembolism (arrow) in a 97-year-old man (PM8). (C) Thrombus in the lung of a 79-year-old woman (PM9) on haematoxylin and eosin staining at 20x magnification; the insert shows CD61 immunohistochemistry indicating moderate staining for platelets. (D) Platelet-rich thrombus in the medium-sized vessels surrounding the heart in a 61-year-old man (PM1); the insert shows strong CD61 staining for platelets. Periodic acid Schiff staining showing a glomerular microaneurysm (arrow, E) and microthrombi within glomerular capillary loops (arrow, F, at 40x magnification) indicative of thrombotic microangiopathy in a 97-year-old man (PM8). Macroscopic splenic (G) and hepatic (H) infarction in a 22-year old man (PM5).

adrenalitis was noted. Two (22%) of nine patients showed chronic inflammation in the thyroid with follicular epithelial cell disruption; however, the significance of this finding is uncertain.

Median combined kidney weight was within normal range, at 264 g (IQR 187–356). Salient renal pathology findings were acute tubular injury in all nine patients, underlying moderate cortical scarring of uncertain cause in one patient (11%), glomerular microaneurysm and thrombi in one patient (11%; figure 2), and rare thrombi in interlobular arteries in four patients (44%). PM6 (24-year-old man) had a higher degree of arterial intimal thickening than expected for that age (appendix p 28). We observed no evidence of focal and segmental glomerulosclerosis, diabetic glomerulopathy, or glomerulonephritis.

Large droplet fatty change was seen in most patients (seven [88%] of eight). Cirrhosis or bridging hepatic fibrosis were noted in three patients (38%). No liver thrombosis was identified histologically, but one patient showed macroscopic liver infarction (figure 2). The median liver weight was 1432 g (IQR 1012–2466) and three (33%) of nine patients showed hepatomegaly (liver weighing >2000 g). Two patients (PM4 and PM7) showed marked autolysis and were not included in analysis.

Moderate to intense microglial activation was the most prominent pathological feature in the CNS (five [100%] of five patients). Mild T-cell infiltration was noted around blood vessels and capillaries in all five patients, but B cells were absent. We found ischaemic changes of variable extent in the neurons of the cortex and in the white matter detected by BAPP (β amyloid precursor protein) stain. However, no necrosis of brain tissue or extensive infiltration of inflammatory cells in brain parenchyma or meninges was observed on histological examination, although one (11%) of nine patients showed macroscopic haemorrhagic transformation in a large recent cerebral infarction in the distribution of the middle cerebral artery.

Tissues from five patients were analysed for presence of viral genomes against *E* gene and indications of viral replication against subgenomic RNA transcripts by qRT-PCR. Viral RNA was present in respiratory tract samples, including lung, of all five cases analysed. In addition, two of three patients had detectable viral RNA in the nasal epithelium and four of five patients in the trachea. Evidence of viral genomes outside the respiratory tract was found for all five patients, but the distribution and viral loads varied case by case (figure 5A). Viral genomes were also detected using a different qRT-PCR targeted at *RdRp* gene, and patterns were consistent between the two sets of primers (data not shown). A third primer set that detected subgenomic RNA indicated virus replication in all tissues examined, with variation between patients in levels and distribution (figure 5B).
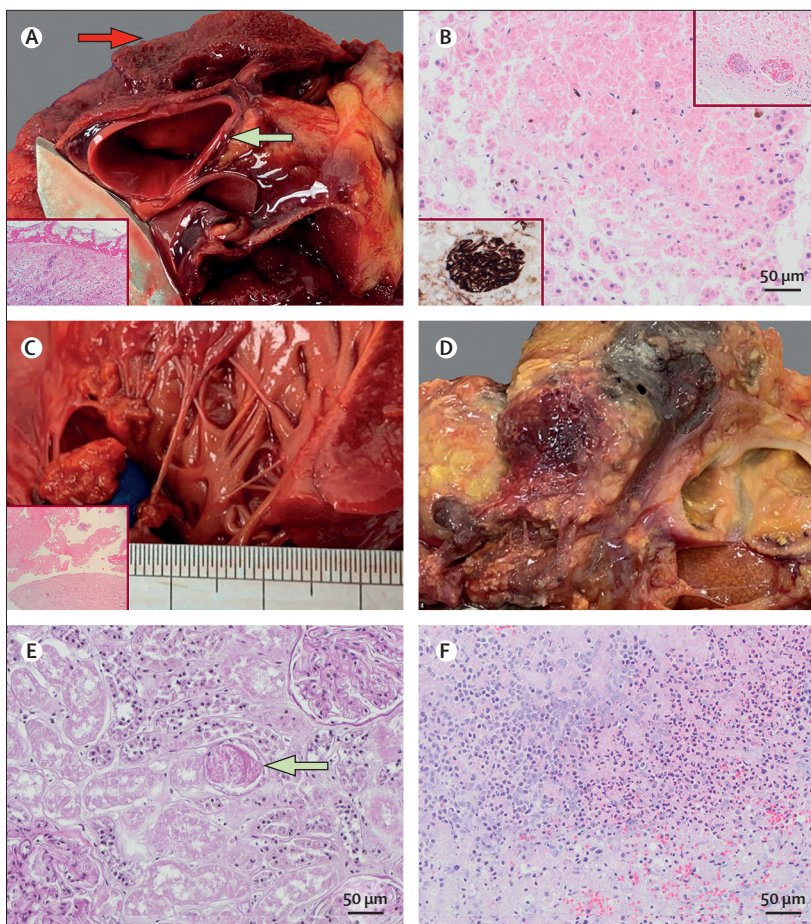

Figure 3: **Other notable autopsy findings in patients with COVID-19**
(A) Contained aortic dissection (green arrow) and fibrinous pericarditis (red arrow) in a 22-year-old man (PM5); insert is a haematoxylin and eosin stain image of the pericardium showing fibrinous pericarditis (10× magnification). (B) Adrenocortical micro-infarcts in a 79-year-old woman (PM9) with re-endothelialising thrombus in small adrenal vessels highlighted by CD34 (insert, bottom left) and haematoxylin and eosin (insert, top right). Marantic endocarditis (C) highlight with haematoxylin and eosin staining (bottom left at 10× magnification) and necrotising, haemorrhagic pancreatitis (D) in a 22-year-old man (PM5) with COVID-19 and a secondary fungal lung infection. (E) Periodic acid Schiff staining showing a granular cast (arrow) indicative of acute tubular injury in a 24-year-old man (PM6; 20× magnification). (F) Microscopic acute pancreatitis on haematoxylin and eosin staining in a 97-year-old man (PM8; 20x magnification).

Discussion

In this series, we have described the major pathological findings identified at autopsy in ten patients who died of severe COVID-19. The most consistent findings were DAD, thrombosis, haemophagocytosis, and immune cell depletion, although unexpected pathologies that are probably related to SARS-CoV-2 infection were also identified.

DAD was the most consistent and prominent feature in our series and others.[7,8] The specific phase of DAD probably represents the degree and chronicity of the offending insult (SARS-CoV-2 infection) in relation to the time of death. This is similar to previous coronavirus epidemics.[6] The conclusion by Copin and colleagues[7] that COVID-19-related lung injury "is not diffuse alveolar damage" might relate to their sampling strategy and
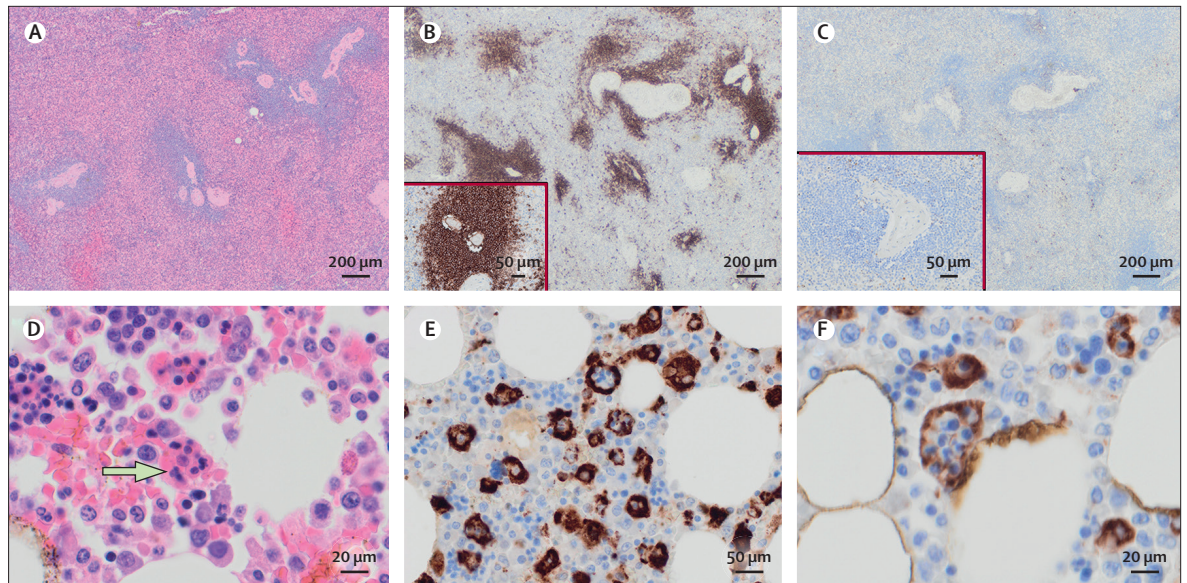
Figure 4: **Pathological findings in haematological organs in patients with COVID-19**
T-cell depletion in the spleen of a 79-year-old woman (PM9) with COVID-19: haematoxylin and eosin staining of the spleen at 10× magnification (A); CD20 staining of spleen indicating presence of B cells (B; 10× magnification), with the insert showing the same region at higher power (20× magnification); and CD3 staining of spleen indicating depletion of T cells (C; 10× magnification), with the insert showing the same region at higher power (20× magnification). Bone marrow phagocytosis in a 97-year-old man (PM8) with COVID-19: haematoxylin and eosin staining of a well preserved bone marrow, with an arrow indicating presence of phagocytosis (D; 40× magnification); and CD68-PGM1 staining of bone marrow indicating presence of phagocytosis (20× [E] and 40× [F] magnification).

chronicity (five patients had spent approximately 3 weeks on a ventilator). Barton and colleagues[8] described prominent acute bronchopneumonia as the major finding in one of two patients, although the authors acknowledge that this was probably affected by aspiration in their patient with muscular dystrophy. Reports of lung histology in early COVID-19 also suggest a degree of lymphocytic pneumonia, although DAD is probably superimposed on this over time in the majority of fatal cases.[7] Pulmonary macrophage infiltration and multinucleated giant cell reactions are prominent, similar to other series.[8–12] Definite evidence of tissue-related lymphocyte depletion in COVID-19 will require quantitative analysis comparing tissues from COVID-19 patients with DAD associated with other conditions and unaffected tissues. Several cases of invasive pulmonary aspergillosis have been reported in patients with severe COVID-19 pneumonia.[18] To our knowledge, this is the first description of histologically proven mucormycosis in patients with COVID-19 and suggests that other human fungal pathogens, including members of Mucoromycotina, can complicate COVID-19-associated infections.

Numerous clinical features, including raised serum D-dimer concentrations, raised pro-calcitonin concentrations, and imaging findings, suggest thrombosis is prominent in patients with COVID-19.[2] Thrombotic features were universal among patients who underwent full autopsies (all nine patients had thrombi in at least one major organ) and have been noted to be prominent in other COVID-19 autopsy series.[15] In a retrospective study of 159 autopsies in patients with acute respiratory distress

syndrome and DAD of various causes, only 24% showed thrombi within the small vessels of the lung despite sampling of every lobe of the lung.[19] Another study used post-mortem angiography and identified thrombi in nearly all cases of acute respiratory distress syndrome from various causes.[20] Whether thrombosis in COVID-19 is more common than in other causes of DAD remains uncertain; however, our data support thrombosis as being a striking feature in these patients. A study suggested endotheliitis as a prominent feature in patients with severe COVID-19,[10] but this was not a prominent feature in our patients. Importantly, limited post mortem or post-mortem cross-sectional imaging are likely to under-represent the true extent of thrombosis (particularly micro-thrombosis) and its impact on patient death. The extent of cardiomegaly, fibro-intimal thickening of renal blood vessels, and obesity in our series supports a contribution of hypertension beyond that noted clinically (only four patients had hypertension documented on the MCCD).

A raised cytokine profile has been documented in a subset of patients with severe COVID-19.[2] Consistent with this, haematological organs in our series showed prominent phagocytosis in several patients, which has not been documented in previous series.[21] Of the four patients with bone marrow haemophagocytosis, one patient (PM7) showed mild transaminitis, hyperbilirubinaemia, elevated serum ferritin concentrations, and fever of 39·1°C; however, most clinical data were insufficient to assess the presence of haemophagocytic lymphohistio-cytosis.

A substantial feature in COVID-19 is lymphocyte depletion, and this is supported in our series by the spleen and lymph node findings. When compared with those with mild disease, patients with severe COVID-19 tend to have a higher neutrophil to lymphocyte ratio and higher CD4-positive to CD8-positive T-cell ratio.[22] Additionally, a negative correlation exists between peripheral blood lymphocyte count and viral copy number.[22] We have corroborated this evidence by documenting a low number of T cells (especially CD8-positive T cells and FOXP3-positive regulatory T cells) in the spleen and lymph nodes in severe fatal COVID-19. Notably, normal plasma cell (both IgM and IgG positive) response was present in haematological organs in most patients.

The extent to which organ-specific pathologies relate to direct viral replication or consequent immunological and cardiovascular complications is of clinical relevance. We report here evidence of viral genomic RNA outside the respiratory tract. This finding is in agreement with several previous studies that have identified viral genomes by qRT-PCR in post-mortem tissues including the colon,[14] spleen,[14] liver,[14,23] skin,[24] heart,[23] and brain.[25] We also report detection of subgenomic RNA, a product that is only produced in actively infected cells. A report identified low viral load in the brain of three of 18 patients with COVID-19, but could not detect the virus in subsequent immunohistochemistry and concluded that the viral genomes might have been present in the blood.[25] Although we cannot exclude that the RNAs detected in our series were similarly carried to the site of sampling in blood, the distribution of RNA in different tissues varied widely between post-mortem cases.

PM3 and PM4 appear to have died earlier in the disease course (<12 days after symptom onset) and had higher viral loads in the respiratory tract than other patients, whereas PM3 and PM4 died after long stays in intensive care units and had either lower overall viral RNA (PM5) or higher viral RNA outside the respiratory tract (PM2). PM1 and PM2 were the only patients in whom we detected viral RNA and subgenomic RNA in the heart and are the only two patients with evidence of acute myocardial injury. Moreover, unlike the previously mentioned study, where virus detected in the brain was 100 000 times less than that detected in the lung, the number of viral genomes detected in external tissues in our series was frequently of similar or even higher levels than that found in the respiratory tree. One study has detected SARS-CoV-2 infection of the endothelium in the vasculature of the skin and lung by immunofluorescent staining for viral antigens.[24] It is not obvious what determines spread and tropism of SARS-CoV-2 outside the respiratory tract. Several studies have reported ACE2 expression levels that were higher in some organs than in others.[26] The sites of highest expression did not correlate with areas of most severe pathological involvement in our series. We should note that cellular receptor status is one of many things that determines the degree of
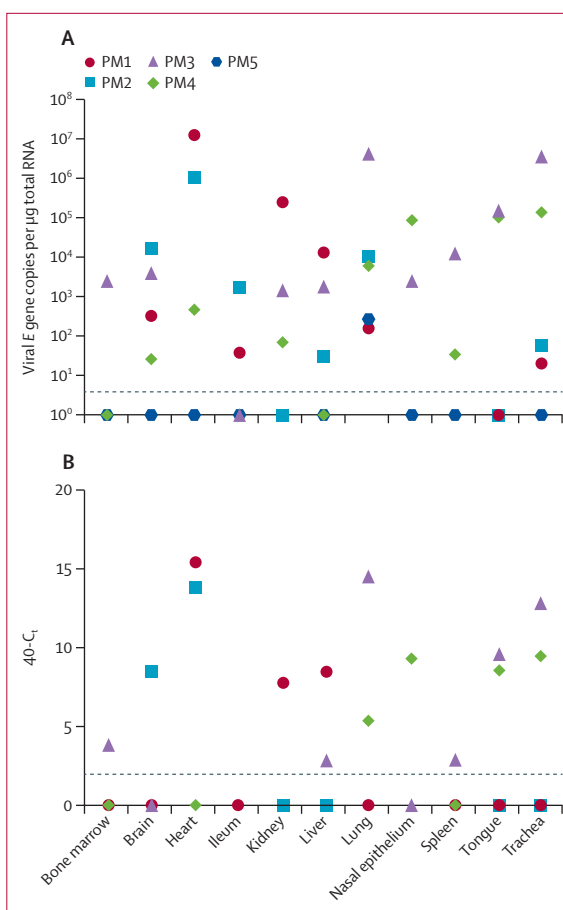

Figure 5: Tissue tropism of SARS-CoV-2 in post-mortem samples
Fresh tissues were collected from a subset of post-mortem examinations and viral load quantified by use of qRT-PCR targeting the viral E gene (A). Detection of viral RNA was verified by use of qRT-PCR against the viral polymerase gene (data not shown). Tissues were additionally tested for subgenomic viral RNA transcripts (B). Dotted lines indicate the limit of detection as ascertained by negative control. Data are included for a 61-year-old man (PM1), a 64-year-old man (PM2), a 69-year-old woman (PM3), a 78-year-old man (PM4), and a 22-year-old man (PM5). qRT-PCR=quantitative RT-PCR. SARS-CoV-2=severe acute respiratory syndrome coronavirus 2.

pathological involvement. Other aspects are likely to play a role, such as route of transmission, acid lability in the stomach, coreceptors, expression of proteases required to activate entry of virus into the cell (eg, TMPRSS2), possibly other yet unidentified host factors, and in-vivo routes of dissemination. The evidence of ongoing replication late in disease supports the use of antiviral therapy even at a point in illness when immunopathology is dominant.

Pancreatic pathology was a major unexpected pathology in this series, which had not been previously reported in COVID-19 autopsies or large clinical COVID-19 series.[2] A 22-year-old man had haemorrhagic, necrotic pancreatitis (PM5). Although this patient also had disseminated mucormycosis, he had evidence of viral persistence in the lung and no fungal hyphae were identified in the pancreas on histological sections. The other patient with

pancreatic pathology had microscopic evidence of pancreatitis that could be missed at autopsy without adequate sampling. The pancreas is a classic site of unexpected pathology identified at autopsy.[27] Serum amylase is not part of the routine care bundle for COVID-19 in our Trust. Whether the pancreatitis was related to SARS-CoV-2 infection or other causes (iatrogenic, comorbidities, or secondary infection) is not clear in our study. Most cases had evidence of hepatic steatosis, which is consistent with clinical findings that obesity is a risk factor for poor outcome in COVID-19, and liver cirrhosis or bridging fibrosis was prominent in this cohort.[28] From these data, nothing suggests direct viral inflammation of the liver.

The interval between time of death and autopsy impaired histological interpretation in many organs and affected antigen preservation. Post-mortem endothelial stripping did affect the endothelial interpretation in our study; however, a substantial number of intact vessels did not show endothelialitis or vasculitis. Additionally, there might be a bias in the cohort, because some religious groups (particularly Jewish and Muslim faiths) will often not give consent for hospital post-mortem examinations. Of note, five of ten patients were of Asian ethnicity in this study, which might be relevant when considering future studies, especially because some ethnicities are reported to have a worse outcome.[29] Possible solutions for these limitations include rapid autopsy examination, limited autopsies, post-mortem cross-sectional imaging, and improved information dissemination in these groups.

Our findings support the role of autopsy in drawing clinicopathological correlations in COVID-19. We have shown pathological evidence of DAD, thrombosis, immune cell depletion, and macrophage activation. Other factors including acute kidney injury, pancreatitis, pericarditis, secondary fungal infections, and pre-existing liver disease require additional investigation. The evidence of ongoing replication late in disease supports the use of antiviral therapy, even at a point in illness when immunopathology is dominant.

Contributors
BH and MO did the autopsies. BH, MO, and GSC designed the study. BH reviewed and compiled the histological findings, prepared the manuscript, took the macrophotographs and microphotographs, collected and analysed the data, and did the literature review. Subspecialist histopathology interpretation and microphotography was done by AGN and PV (lung pathology), KNN (haematopathology), RG (liver pathology), JW (head and neck pathology), CR (renal pathology), and SA-S (neuropathology). OCS, LB, RP, and WSB did the viral studies. OCS prepared sections of the manuscript related to viral tropism. BH collected clinical data, and GSC, PM, MT, and RC assisted in ultrasound-guided biopsy sampling in the limited post mortem. BH, CR, KNN, RG, GSC, MT, RC, AGN, OCS, WSB, PV, and MO reviewed the manuscript.

Declaration of interests
We declare no competing interests.

References
1 European Centre for Disease Prevention and Control. Threats and outbreaks: COVID-19. 2020. https://www.ecdc.europa.eu/en/novel-coronavirus-china (accessed Aug 5, 2020).
2 Huang C, Wang Y, Li X, et al. Clinical features of patients infected with 2019 novel coronavirus in Wuhan, China. *Lancet* 2020; 395: 497–506.
3 Hanley B, Lucas SB, Youd E, Swift B, Osborn M. Autopsy in suspected COVID-19 cases. *J Clin Pathol* 2020; 73: 239–42.
4 Ferrario CM, Jessup J, Chappell MC, et al. Effect of angiotensin-converting enzyme inhibition and angiotensin II receptor blockers on cardiac angiotensin-converting enzyme 2. *Circulation* 2005; 111: 2605–10.
5 Hoffmann M, Kleine-Weber H, Schroeder S, et al. SARS-CoV-2 cell entry depends on ACE2 and TMPRSS2 and is blocked by a clinically proven protease inhibitor. *Cell* 2020; 181: 271–80.
6 Gu J, Korteweg C. Pathology and pathogenesis of severe acute respiratory syndrome. *Am J Pathol* 2007; 170: 1136–47.
7 Copin MC, Parmentier E, Duburcq T, Poissy J, Mathieu D. Time to consider histologic pattern of lung injury to treat critically ill patients with COVID-19 infection. *Intensive Care Med* 2020; 46: 1124–26.
8 Barton LM, Duval EJ, Stroberg E, Ghosh S, Mukhopadhyay S. COVID-19 autopsies, Oklahoma, USA. *Am J Clin Pathol* 2020; 153: 725–33.
9 Sapino A, Facchetti F, Bonoldi E, Gianatti A, Barbareschi M, on behalf of Società Italiana di Anatomia Patologica e Citologia S. The autopsy debate during the COVID-19 emergency: the Italian experience. *Virchows Arch* 2020; 476: 821–23.
10 Varga Z, Flammer AJ, Steiger P, et al. Endothelial cell infection and endotheliitis in COVID-19. *Lancet* 2020; 395: 1417–18.
11 Zhang H, Zhou P, Wei Y, et al. Histopathologic changes and SARS-CoV-2 immunostaining in the lung of a patient with COVID-19. *Ann Intern Med* 2020; 172: 629–32.
12 Tian S, Hu W, Niu L, Liu H, Xu H, Xiao S-Y. Pulmonary pathology of early phase 2019 novel coronavirus (COVID-19) pneumonia in two patients with lung cancer. *J Thorac Oncol* 2020; 15: 700–04.
13 Ackermann M, Verleden SE, Kuehnel M, et al. Pulmonary vascular endothelialitis, thrombosis, and angiogenesis in COVID-19. *N Engl J Med* 2020; 383: 120–28.
14 Adachi T, Chong JM, Nakajima N, et al. Clinicopathologic and immunohistochemical findings from autopsy of patient with COVID-19, Japan. *Emerg Infect Dis* 2020; published online May 15. https://doi.org/10.3201/eid2609.201353.
15 Dolhnikoff M, Duarte-Neto AN, de Almeida Monteiro RA, et al. Pathological evidence of pulmonary thrombotic phenomena in severe COVID-19. *J Thromb Haemost* 2020; 18: 1517–19.
16 Corman VM, Landt O, Kaiser M, et al. Detection of 2019 novel coronavirus (2019-nCoV) by real-time RT-PCR. *Euro Surveill* 2020; 25: 2000045.
17 Wölfel R, Corman VM, Guggemos W, et al. Virological assessment of hospitalized patients with COVID-2019. *Nature* 2020; 581: 465–69.
18 Lahmer T, Rasch S, Spinner C, Geisler F, Schmid RM, Huber W. Invasive pulmonary aspergillosis in severe COVID-19 pneumonia. *Clin Microbiol Infect* 2020; published online June 2. https://doi.org/10.1016/j.cmi.2020.05.032.

19   Thille AW, Esteban A, Fernández-Segoviano P, et al. Chronology of histological lesions in acute respiratory distress syndrome with diffuse alveolar damage: a prospective cohort study of clinical autopsies. *Lancet Respir Med* 2013; **1:** 395–401.

20   Tomashefski JF Jr, Davies P, Boggis C, Greene R, Zapol WM, Reid LM. The pulmonary vascular lesions of the adult respiratory distress syndrome. *Am J Pathol* 1983; **112:** 112–26.

21   Menter T, Haslbauer JD, Nienhold R, et al. Postmortem examination of COVID-19 patients reveals diffuse alveolar damage with severe capillary congestion and variegated findings in lungs and other organs suggesting vascular dysfunction. *Histopathology* 2020; published online May 4. https://doi.org/10.1111/his.14134.

22   Hanley B, Roufosse CA, Osborn M, Naresh KN. Convalescent donor SARS-CoV-2-specific cytotoxic T lymphocyte infusion as a possible treatment option for COVID-19 patients with severe disease has not received enough attention till date. *Br J Haematol* 2020; **189:** 1062–63.

23   Tian S, Xiong Y, Liu H, et al. Pathological study of the 2019 novel coronavirus disease (COVID-19) through postmortem core biopsies. *Mod Pathol* 2020; **33:** 1007–14.

24   Magro C, Mulvey JJ, Berlin D, et al. Complement associated microvascular injury and thrombosis in the pathogenesis of severe COVID-19 infection: a report of five cases. *Transl Res* 2020; **220:** 1–13.

25   Solomon IH, Normandin E, Bhattacharyya S, et al. Neuropathological features of Covid-19. *N Engl J Med* 2020; published online June 12. https://doi.org/10.1056/NEJMc2019373.

26   Li M-Y, Li L, Zhang Y, Wang X-S. Expression of the SARS-CoV-2 cell receptor gene ACE2 in a wide variety of human tissues. *Infect Dis Poverty* 2020; **9:** 45.

27   Wilson C, Imrie CW. Deaths from acute pancreatitis: why do we miss the diagnosis so frequently? *Int J Pancreatol* 1988; **3:** 273–81.

28   Hu L, Chen S, Fu Y, et al. Risk factors associated with clinical outcomes in 323 COVID-19 hospitalized patients in Wuhan, China. *Clin Infect Dis* 2020; published online May 3. https://doi.org/10.1093/cid/ciaa539.

29   Khunti K, Singh AK, Pareek M, Hanif W. Is ethnicity linked to incidence or outcomes of COVID-19? *BMJ* 2020; **369:** m1548.